

Synthesis and characterization of size tuned CdS Quantum dots

Dr Jyotsna Chauhan*, Dr varsha Rani Mehto, Deepika Soni

*HOD Department of Nanotechnology, Rajiv Ganhi Technical University, Bhopal (M.P.), India

*Corresponding authors E-mail- jyotsnachauhan2006@gmail.com

Abstract: CdS nanoparticles are synthesized using chemical precipitation at room temperature. Cadmium sulfide is one of the most promising materials for solar cells and of great interest for their practical applications in up to electronics and photonics. The optical properties get modified due to the confinement of charge carrier within the nanoparticles. The physical and chemical properties of thus nanoparticles are found to be size dependent. The crystallite sizes of cadmium sulfide crystals were estimated from the peaks of XRD. The optical properties of the samples were estimated by UV visible spectroscopy. The functional groups present in the synthesized CdS materials are identified by FTIR analysis. XRD is used to carry out the structural characterization of the nanoparticles. The coloration of the nanoparticle is directly linked to the band gap. The color of the emitted light depends on the size of the quantum dots, the larger the quantum dots size, the redder the light.

[Dr Jyotsna Chauhan, Dr varsha Rani Mehto, Deepika Soni. **Synthesis and characterization of size tuned CdS Quantum dots.** *Rep Opinion* 2017;9(10):84-93]. ISSN 1553-9873 (print); ISSN 2375-7205 (online). <http://www.sciencepub.net/report>. 15. doi:[10.7537/marsroj091017.15](https://doi.org/10.7537/marsroj091017.15).

Keywords: XRD; FTIR; UV; chemical precipitation method

1. Introduction

CdS has promising applications in multiple technical fields including photochemical catalysis, gas sensor, detectors for laser and infrared, solar cells, nonlinear optical materials, various luminescence devices, optoelectronic devices and so on [1–2]; it is also most promising candidate among II-VI compounds for detecting visible radiation [10]. CdS can be obtained in thin film form, by various methods [4–5] or in powder form, by hydrothermal/solvothermal methods, thermal decomposition etc. [3, 6 7]. In last decades, efforts have been devoted to the preparation of high - quality CdS nanoparticles and the investigation of optical properties. [8] The possibility of tuning the properties of particles by controlling their sizes and shapes implies search of new experimental methodologies that yield very low size- and shape-dispersion nanoparticles. For example, sea-urchin like cadmium sulfide nanoparticles with nanorod-based architecture were prepared by solvothermal method, with cadmium chloride and thiourea in ethylenediamine solution [9]; the CdS nanoparticles have been assembled into CdS nanorods and arrayed nanorod bundles by a thioglycolic acid [10]; cadmium sulfide nanorods were also synthesised in micro-emulsions formed by non-ionic surfactants [11]. There are many reports about cadmium sulfide nanoparticles, obtained by different methods and from different precursors. [11 - 13].

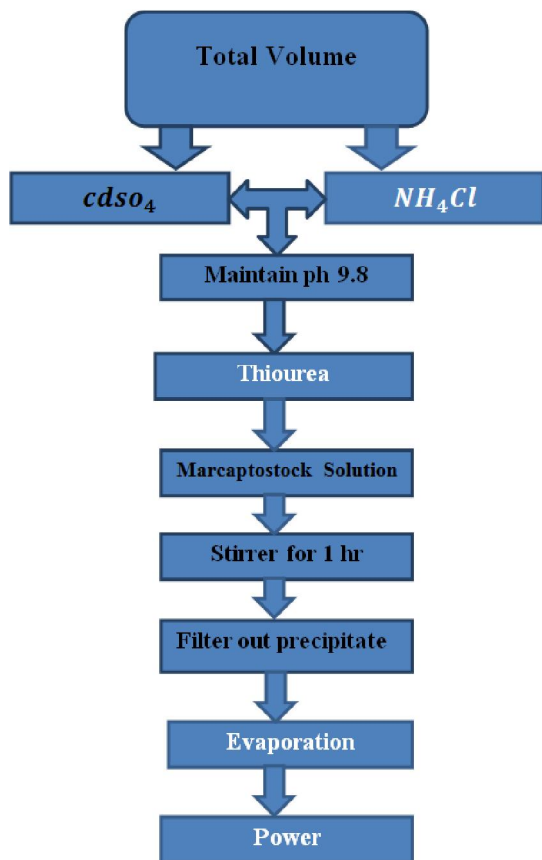
In the present work describes synthesis and characterization of cadmium sulfide using chemical precipitation techniques. Different sizes of CdS nanoparticles were obtained by using different concentration of Mercaptoethanol. Enhanced structural

and optical properties were obtained with decreasing the size of CdS nanoparticles.

Experimental:-

CdS nanoparticles are prepared by the colloidal chemical precipitation method using cadmium sulphate (CdSO_4), Ammonium chloride (NH_4Cl) and thiourea in molar ratio of 1:3:7. Mercapto ethanol is used as capping agent.

These compounds are weighed in a microbalance (M/s SICO, India). on 100 ml volume we take 90ml water and keep it on stirrer after mixing the cadmium sulphate (CdSO_4), and Ammonium chloride (NH_4Cl) after than maintain the ph of solution at 9.8 by the help of ammonia NH_3 than mix the (2ml,4ml,8ml) mercapto stock solution (4ml mercapto + 96ml DIwater) and lastly mix the thiourea as A supporting electrolyte. and the flask was constantly stirred for about 1 hours at room temp. Then the precipitates were filtered out. The structure and phase of the sample are determined by X-ray diffraction Technique (XRD) Diffraction patterns have been recorded over the range of 20– 80 at the scan rate of 2 degree/min. CdS nanoparticles have been synthesized by aqueous medium through chemical co-precipitation technique. X-ray diffraction measurement confirms the structure, single phase cubic and particle size 10 nm for the sample CdS Bulk, 1.98 nm for sample CdS 8ml and 2.64nm for sample CdS 4ml. The Optical properties were determined by using UV-Vis spectroscopy, Structural and Morphological properties were analyzed by Fourier Transform Infrared Spectroscopy (FTIR), X-Ray Diffraction (XRD) and Scanning Electron Microscopy (SEM).



2. Result and Discussion

2.1. Structural Properties of CdS by X-ray Diffraction Analysis:-

XRD pattern provide information about crystalline phase of the nanoparticles as well as the crystallite size. A considerable broadening of diffraction peaks is the characteristic feature of the x-ray diffraction patterns of films and ultra-dispersed powders of cadmium sulfide. This broadening of the diffraction peaks is associated with the small sizes of particles in powders.

Fig 1, 2 and 3 shows the XRD pattern of sample CdS1, CdS2 and CdS3 respectively. X-ray diffraction studies confirmed that the synthesized materials were CdS with **cubic phase** and the entire diffraction peak agreed with the reported JCPDS data. Comparing with the data of the JCPDS file (Powder Diffraction File Card, No. 10-0454), it was found that the CdS nanoparticles are identified as β-CdS, which belong to the cubic crystal system. The XRD peaks are found to be broad indicating fine size of the sample grains. The XRD pattern of a typical CdS sample exhibits peaks at 2θ values of 26.67°, 43.98° and 51.89° which could be indicated as scattering from the (111), (220), and (311) cubic phase CdS plans, respectively, suggesting that the nanoparticles are in cubic (Zinc blend phase) form and are in good agreement with the reported data on

CdS (Rodríguez et al., 2008; Wang et al., 2001). The broadening of the diffraction peak provides information about crystallite size. As the width increases, the particle size decreases and vice versa (Banerjee et al., 2000).

The X-ray diffraction data were recorded by using Cu Kα radiation (1.5406 Å). The average grain size was calculated with the help of Scherrer equation using the diffraction intensity of the peak that has highest intensity.

Scherrer equation is

$$D = 0.89\lambda / (\beta \cos\theta) \dots \dots \dots (1)$$

Where D is the grain size, λ is the wavelength of x-ray radiation, β is the full width at the half maximum (FWHM) of the CdS nanoparticles and θ is the diffraction angle. Standard data is taken from the JCPDS card No. 36-1451. The Calculated grain size using the peak (111) were found 10, 2.64 and 1.98 nm for sample CdS1, CdS2 and CdS3 respectively using the Scherrer eq. The summary of XRD parameters are given in table 1.

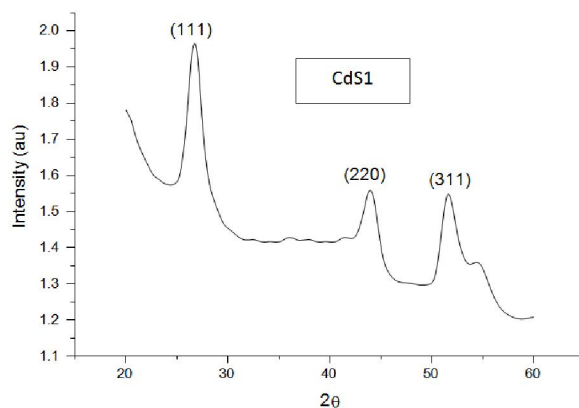


Figure.1 XRD Pattern of CdS1 Quantum dots with grain size 10nm

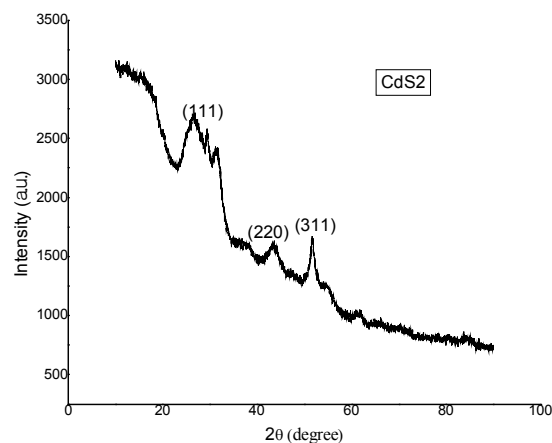
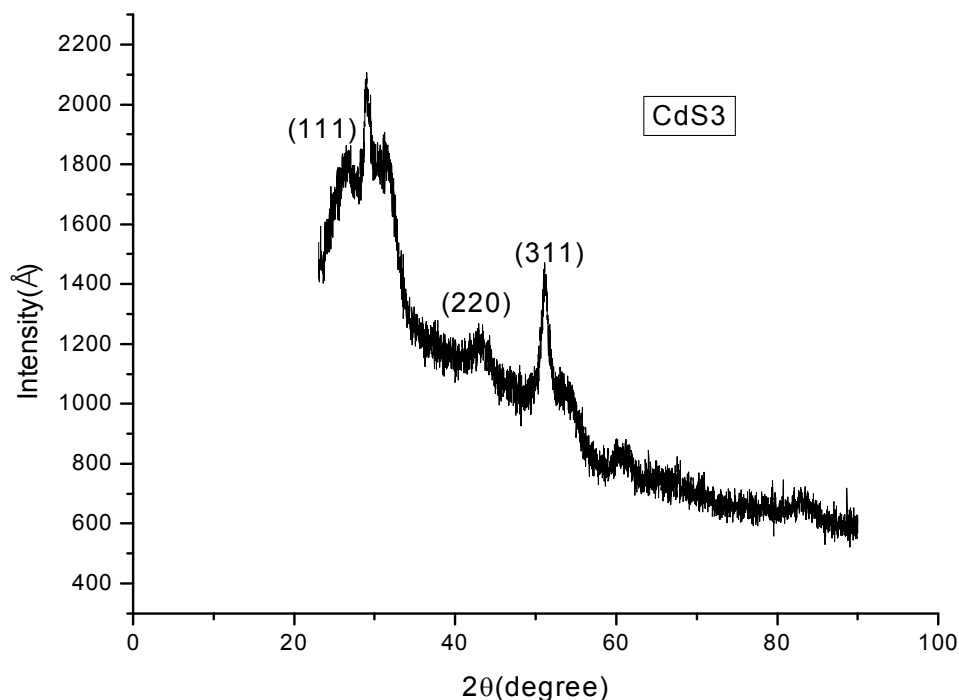


Figure.2 XRD Pattern of CdS2 Quantum dots with grain size 2.64 nm

Table No. 01 from XRD analysis of Size Tuned CdS Quantum dots

Sample	FWHM (A ⁰)	Peak No	2θ (degree)	h k l	Inter planar spacing d values (A ⁰)		Intensity (A ⁰)		Grain Size (nm)
					Standard d (A)	Observed d (A)	Standard	Observed	
CdS1	0.85625	1	26.69	1 1 1	3.36	3.3360	100	100	10
		2	43.98	2 2 0	2.06	2.0563	40	39	
		3	51.82	3 1 1	1.75	1.7621	60	58	
CdS2	3.05777	1	26.62	1 1 1	3.36	3.34463	100	100	2.64
		2	43.69	2 2 0	2.06	2.06935	40	37	
		3	51.72	3 1 1	1.75	1.76531	60	58	
CdS3	4.0786	1	26.69	1 1 1	3.36	3.3360	100	100	1.98
		2	43.98	2 2 0	2.06	2.0563	40	35	
		3	51.82	3 1 1	1.75	1.7621	60	56	

**Figure 3. XRD Pattern of CdS3 Quantum dots with grain size 1.98 nm****2.2. Texture Coefficient:-**

In material science, texture is the distribution of crystallographic orientations of a polycrystalline sample. Material properties such as strength, chemical reactivity, stress corrosion, cracking resistance, weld ability, deformation behavior, resistance to radiation damage and magnetic susceptibility can be highly dependent on the material texture and related changes in microstructure. Quantitative information concerning the preferential crystal orientation can be obtained from the texture coefficient, TC, defined as.

$$Tc(hkl) = \frac{I(hkl)}{I_o(hkl)} \left\{ \frac{1}{n} \sum \frac{I(hkl)}{I_o(hkl)} \right\}^{-1}$$

Where $TC(hkl)$ is the texture coefficient, $I(hkl)$ is the XRD intensity and n is the number of diffraction peaks considered. $I_o(hkl)$ is the intensity of the XRD reference of the randomly oriented grains. As $TC(hkl)$ increases, the preferential growth of the crystallites in the direction perpendicular to the hkl plane is greater.

A summary of Texture coefficient is given in Table 02. Texture coefficient for the peak (111) is highest that shows intensity of that peak is high and that is most preferable peak for the XRD calculation, texture coefficient shows tendency to orientation in the (111) plane. Values higher than 1 indicate the abundance of grains in a given (hkl) directions. All the peaks are not suited for particle size calculation.

Table No. 02 from Texture Coefficient of Size Tuned CdS Quantum dots

Sample	FWHM (A^0)	Peak No	h k l	Intensity (A^0)		TC (hkl)	Grain Size (nm)
				Standard I_0 (hkl)	Observed I (hkl)		
CdS1	0.85625	1	1 1 1	100	100	1.037	10
		2	2 2 0	40	37	0.959	
		3	3 1 1	60	58	0.988	
CdS2	3.05777	1	1 1 1	100	100	1.035	2.64
		2	2 2 0	40	37	0.963	
		3	3 1 1	60	58	0.988	
CdS3	4.0786	1	1 1 1	100	100	1.068	1.98
		2	2 2 0	40	35	0.934	
		3	3 1 1	60	56	0.988	

2.3. Optical Properties Of CdS By UV-Vis Absorption Analysis:-

Quantum dots are semiconductors whose electronic characteristics are closely related to the size and shape of the individual crystal. Generally, the smaller the size of the crystal, the larger will be the band gap, and greater will be the difference in energy between the highest valence band and the lowest conduction band. Therefore more energy is needed to excite the dot, and concurrently, more energy is released when the crystal returns to its resting state. Due to quantum size effect, as the radius of the crystallite approaches the Bohr radius of an exciton, the energy gap begins to widen, quantization of the energy bands becomes apparent and a blue shift in the exciton transition energy can be observed [14 -17]. The effective mass model is commonly used to study the size dependence of optical properties of Quantum Dotssystem [18]. CdS shows variation in 1D morphology when the reaction conditions change (i.e. monomer concentration, reaction temperature and reaction time). Any combination of reaction conditions could lead to diverse shapes such as dots, rods, bipods, tripods, tetrapods and spindles [19, 20].

As CdS nanoparticles (quantum dots) has wide band gap, it is widely used in optoelectronics, photonics, photovoltaics and photocatalysis. It is used as window material for hetero junction solar cells to avoid the recombination of photogenerated carriers which consequently improves the solar cells efficiency [21]. In optoelectronics, it is utilized for making photocells, light emitting diode (LED) [22 23], lasers [24], and address decoders [25]. In photonics, CdS is employed to make nanocrystals [26], sensors [27], optical filters, and all optical switches [28]. In photovoltaics, it has been exploited to fabricate cadmium telluride (CdTe), as well as copper indium diselenide solar cells to act as a window layer that separates charge carriers produced due to photon absorption and photo detectors [29] and in the

fabrication of thin film solar cells [30,31]. In photocatalysis, it is used for hydrogen production [32] and water purification [33]. CdS is also used as a pigment in paints and in engineered plastic for good thermal stability [40]. These properties are the result of high surface-to-volume ratio present in CdS nanoparticles. In the present work, CdS nanoparticles were synthesized by single pot chemical precipitation method in aqueous medium using ambient reaction conditions using ambient reaction conditions. The Optical properties were determined by using UV-Vis spectroscopy.

The UV-Vis spectroscopy has become an effective tool in determining the size and optical properties. The optical properties were determined by using Thermo Spectronics, Genesis 20 Spectrometer in the wavelength range of 400-600 nm at room temperature using the stable dispersions formed in DMSO after ultra-sonication. As the particle size decreases, the λ max shifts to shorter wavelengths, due to the band gap increase of the smaller-sized particles [23, 41]. The nature of the electronic transition across the optical band gap is determined by the variation of optical coefficient with wavelength. The nature of the transition is

Determine using the relation [42]:

$$(\alpha h\nu) = A(h\nu - E_g)^n \dots \dots \dots (1)$$

Where ' α ' is the absorption coefficient, 'A' is a constant related to the effective masses associated with the bands, ' $h\nu$ ' is the energy of photon and $n=1/2$ for allowed direct transition. The value of absorption coefficient is found to be of the order of 10^4 cm^{-1} for all composition that supports the direct band gap nature of the semiconductor [34]. The most direct way of extracting the optical band gap is to simply determine the wavelength at which the extrapolations of the base line and the absorption edge cross [35, 36]. With the band gap value, the particle radius can be calculated using equation proposed by Brus [37,38]. The Brus equation is used to describe the emission

energy of quantum dot semiconductor nanocrystals. This expression gives a relation between radius of the crystallite and the energy gap thus explains the quantum size effect.

$$E_g = E_{g0} + \frac{(\hbar\pi)^2}{2R^2} \left[\frac{1}{m_e} + \frac{1}{m_h} \right] - 1.786 \frac{e^2}{\epsilon R} - 0.248 E_{ry} \dots \dots \dots (2)$$

Where; E_g is the band gap value of the nanoparticles, E_{g0} is the band gap value of the bulk material, m_e and m_h are effective masses of electrons and holes, respectively. ϵ is the dielectric constant of the semiconductor, R is the radius of the particle; h is the plank constant and E_{ry} is the effective Rydberg energy [39]. The first term in Equation (2) referred to

as the quantum localization term (i.e. the kinetic energy term), which shifts the E_g to higher energies proportionally to R^{-2} . The second term in Equation (2) arises due to the screened coulomb interaction between the electron and hole, it shifts the E_g to lower energy as R^{-1} . The third, size independent term in Equation (2) is the solvation energy loss and is usually small and ignored. In case of semiconductors the effect of the second term, the coulomb interaction term in the equation (2) is very less and hence can be ignored as well. [40, 41].

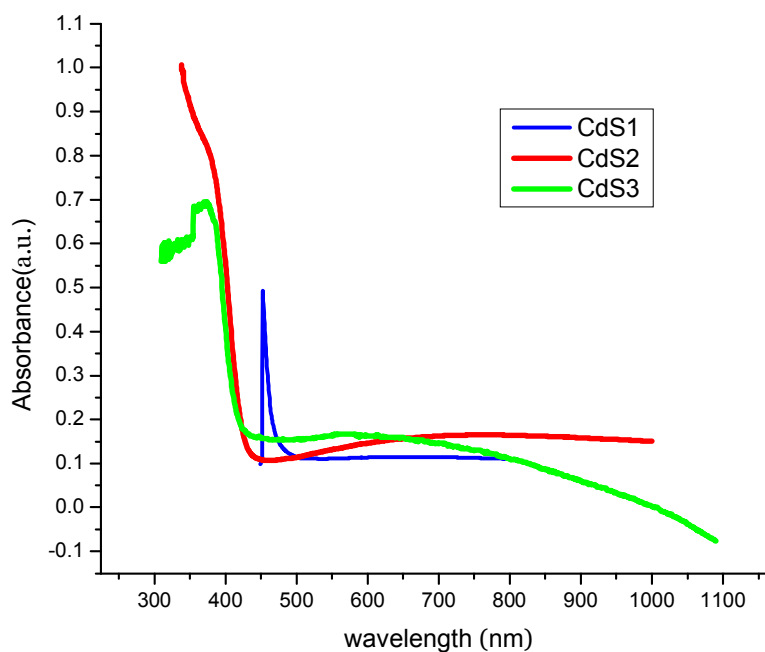


Figure 4. UV-Vis Absorption Pattern of Size Tuned CdSQdots

The reported value of absorption edge in bulk CdS was found at 515 nm while in prepared CdS nanoparticles the absorption peaks were observed at 451.84, 339.79 and 315.74 nm for CdS1, CdS2 and CdS3 respectively; wavelength (fig 4) which indicates the blue shift in absorption edge. Absorption peak shows shift to shorter wavelength (blue shift) with decreasing the size, which is in good agreement with the results reported [42]. Graph shows the plot of Absorbance versus $h\nu$ whose intercept on energy axis gives the band gap energy E_g of the particles which came out to be 2.74 eV, 3.65 eV and 3.94 eV for CdS1, CdS2 and CdS3 respectively (reported standard value of band gap for bulk CdS = 2.42 eV). The summary of UV visible parameters is given in table 03.

The particle size of the synthesized CdS nanoparticles was calculated from Equation (2) keeping $E_{g0} = 2.42$ eV, $m_e = 1.73 \times 10^{-19}$, $m_h = 7.29 \times 10^{-19}$, for CdS, and $E_g = 2.74, 3.65, 3.94$ eV

(observed) (graph). The particle size came out to be nm. The prepared CdS nanoparticles had wider band gap than the bulk CdS due to quantum size effect, and can be used in optoelectronics, photonics, photo voltaics, photo catalysis and solar cells.

The above graph shows that even for those photons which have an energy above the band gap, the absorption coefficient is not constant, but still depends strongly on wavelength. The probability of absorbing a photon depends on the likelihood of having a photon and an electron.

Different semiconductor materials have different absorption coefficients. Materials with higher absorption coefficients more readily absorb photons, which excite electrons into the conduction band. Knowing the absorption coefficients of materials aids engineers in determining which material to use in their solar cell designs.

The absorption coefficient determines how far into a material light of a particular wavelength can penetrate before it is absorbed. In a material with a low absorption coefficient, light is only poorly absorbed, and if the material is thin enough, it will appear transparent to that wavelength. The absorption coefficient depends on the material and also on the wavelength of light which is being absorbed. Semiconductor materials have a sharp edge in their absorption coefficient, since light which has energy below the band gap does not have sufficient energy to excite an electron into the conduction band from the valence band. Consequently this light is not absorbed. The absorption coefficient for several semiconductor materials is shown below. The above graph shows that even for those photons which have energy above the band gap, the absorption coefficient is not constant, but still depends strongly on wavelength. The probability of absorbing a photon depends on the likelihood of having a photon and an electron interact in such a way as to move from one energy band to

another. For photons which have energy very close to that of the band gap, the absorption is relatively low since only those electrons directly at the valence band edge can interact with the photon to cause absorption. As the photon energy increases, not just the electrons already having energy close to that of the band gap can interact with the photon. Therefore, a larger number of electrons can interact with the photon and result in the photon being absorbed. The energy gap values depends in general on the films crystal structure, the arrangement and distribution of atoms in the crystal lattice, also it is affected by crystal regularity. The energy gap (E_g) value is calculated by extrapolation of the straight line of the plot of $(\alpha h\nu)^2$ versus $(h\nu)$ photon energy for different deposition parameters the linear dependence of $(\alpha h\nu)^2$, $(h\nu)$ with indicates direct band gap. The band gap increases with the increase in thiourea ion concentration. More probably this is related to the decrease in grain size with increasing deposition rate.

Table No. 03 from UV Visible Absorption analysis of Size Tuned CdS Quantum dots

Sample Name	Wavelength (λ) at absorption peak (nm)	Experimental Band gap E_g (eV)	Theoretical EMA Band gap E_g (eV)	Theoretical TBT Band gap E_g (eV)	Particle size (nm)
CdS1	451.843	2.74	2.75	3.11	10
CdS2	339.793	3.65	3.18	3.57	2.64
CdS3	315.737	3.93	3.87	3.78	1.98

The UV absorbance spectral presented in the figures above reveal that as the size of the Nano crystals shrink, the maximum peak shifted to a shorter wavelength leading to corresponding increase in the confinement energies because the valence band is move downward and conduction band is pushed upward thus widening the band gap of the semiconductor Nano crystals. The net effect is that the band gap increases. This results to a blue-shift of the (band-band) excitation energy of the semiconductor. The value of the band gaps of the various synthesized nanoparticles was quite large when compared to typical band gap in bulk CdS. This rapid increase in band gap and shift in the electron transition to higher energies with decreasing dot size is due to enhancement in surface/volume ratio and accompanied increase in oscillation strength of the Nano crystal induced by the quantum size effect (QSE). Ashcroft, N.W. AND Mermin, (1976).

2.4. Optical Properties of CdS By Photoluminescence Analysis:-

Special interest in quantum dots is due to a considerable difference between the discrete exciton spectrum of the quantum dots and the spectrum of a bulk crystal of the same chemical

Composition. This difference leads to a change in the optical properties of quantum dots as compared to the bulk material. In particular, the emission band of the quantum dots can be located, depending on their size, in any part of the spectrum from the ultraviolet to infrared range [48, 49]. This makes it possible to produce markers of various color for optical coding [50] and to use quantum dots in opto electronics [51] and for studying the structure of biological cells and influence of various factors on the cells [52, 53].

The photoluminescence spectrum of CdS quantum dots was measured by photoluminescence spectroscopy. The wavelength of the excitation light was 320 nm. The spectrum included a pretty narrow photoluminescence peak with the maximum at about 477.187, 451.307 and 423.453nm for CdS1, CdS2 and CdS3 respectively. And shifted towards blue side with decreasing in size. (shown in fig 5)

An immediate optical feature of the quantum dots synthesize is their color. Although the quantum dots were of the same material but their different sizes results to emission of light of different colors. The larger the QDT size, the redder (lower its fluorescence spectrum). Conversely, smaller (QDTs) emit bluer (higher energy) light. The colorations is directly

related to the energy levels of the quantum dot. Quantitatively speaking, the band gap energy determined the energy (and hence color) of the fluorescence light which is inversely proportional to the size of the quantum dot. The material properties changes dramatically because the quantum size effect arises from the confinement of the electrons and holes in the material. The increased surface area/volume ratio and accompanied increase in oscillator strength as a result of the downsizing the bulk CdS to nanometer range is responsible for the unprecedented increase in the band gap of the synthesized nanoparticle over their bulk counterpart. The summary of PL parameters is given in table 04.

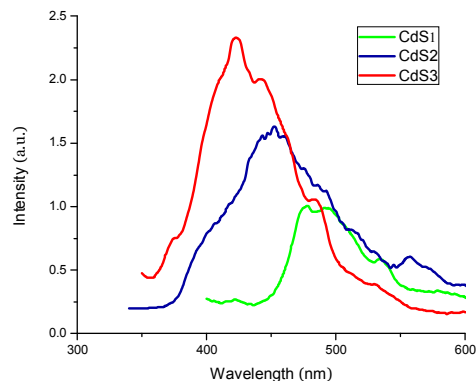


Figure 5 Photoluminescence Pattern of Size Tuned CdS Quantum dots

Table No. 04 from PL analysis of Size Tuned CdS Quantum dots

Sample Name	Particle Size (nm)	Capping Agent Volume (Mercapto stock solution in ml)	PL Peak Position
CdS1	10	2ml	477.187
CdS2	2.64	4ml	451.307
CdS3	1.98	8ml	423.453

2.5. Fourier Transform Infrared Spectroscopy (FTIR)

Another method to study the purity and composition of the products is FTIR. The dried CdS nanoparticles were characterized with FTIR. The functional groups present in the as-synthesized materials are identified by FTIR analysis.

Sophisticated Analytical Instrumental Laboratory,
School of Pharmaceutical Sciences, RGPV, Bhopal.

SHIMADZU

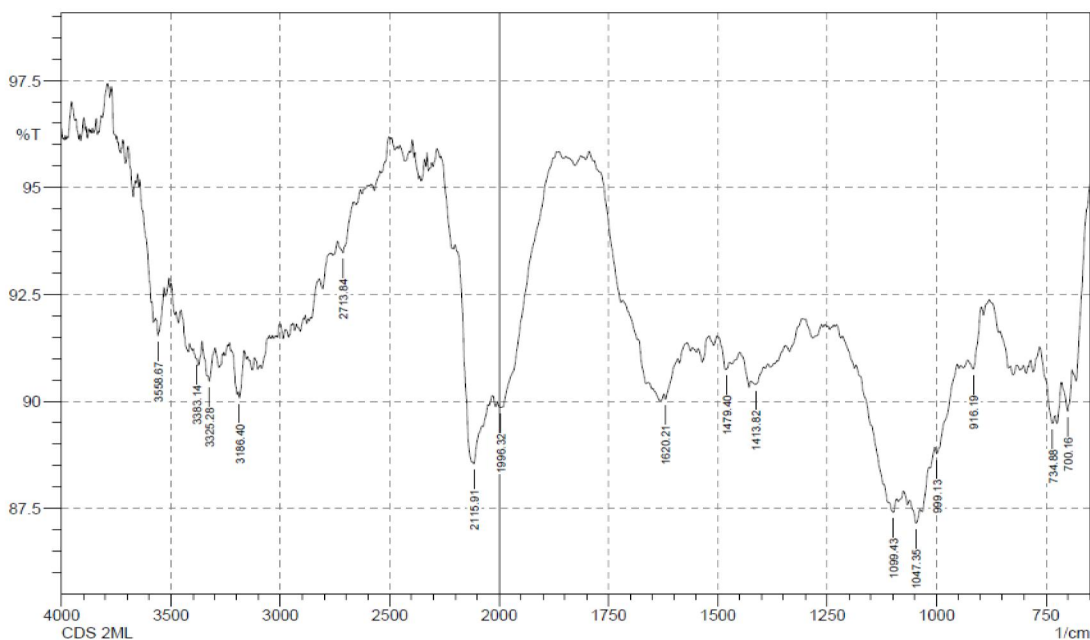


Figure 6.1FTIR Pattern of CdS1 Quantum dots

FT-IR spectrum of CdS film is presented in figure6, the band at 3558.68 cm^{-1} is due to O-H stretching vibrations of water molecules. The bending vibrations of C=N appeared at 1620.21 cm^{-1} . CdS particles showed two stretching bands of C-O at 1099.43 cm^{-1} . At 700.42 cm^{-1} and 734.36 cm^{-1} , there are medium to strong bands which have been assigned to Cd-S stretching.

Sophisticated Analytical Instrumental Laboratory,
School of Pharmaceutical Sciences, RGPV, Bhopal.

SHIMADZU

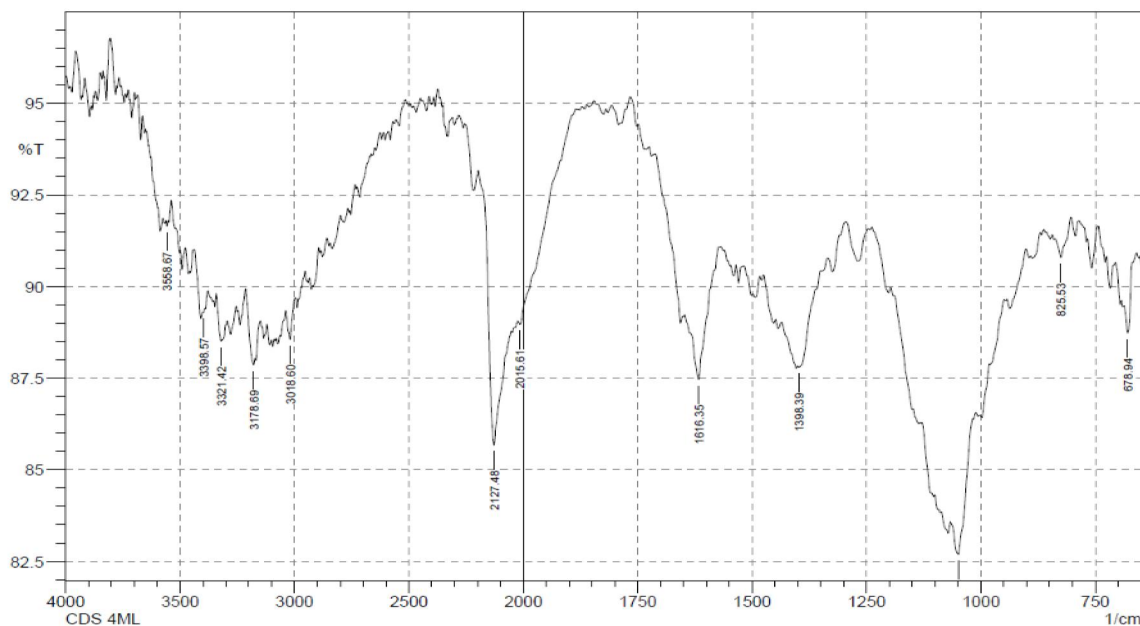


Figure 7 FTIR Pattern of CdS2 Quantum dots

FT-IR spectrum of CdS film is presented in figure 7 the band at 3558.67cm^{-1} is due to O-H stretching vibrations of water molecules. The bending vibrations of C=N appeared at 1616.35cm^{-1} . CdS particles showed two stretching bands of C-O at 1049.28cm^{-1} . At 678.94cm^{-1} and 825.53cm^{-1} , there are medium to strong bands which have been assigned to Cd-S stretching.

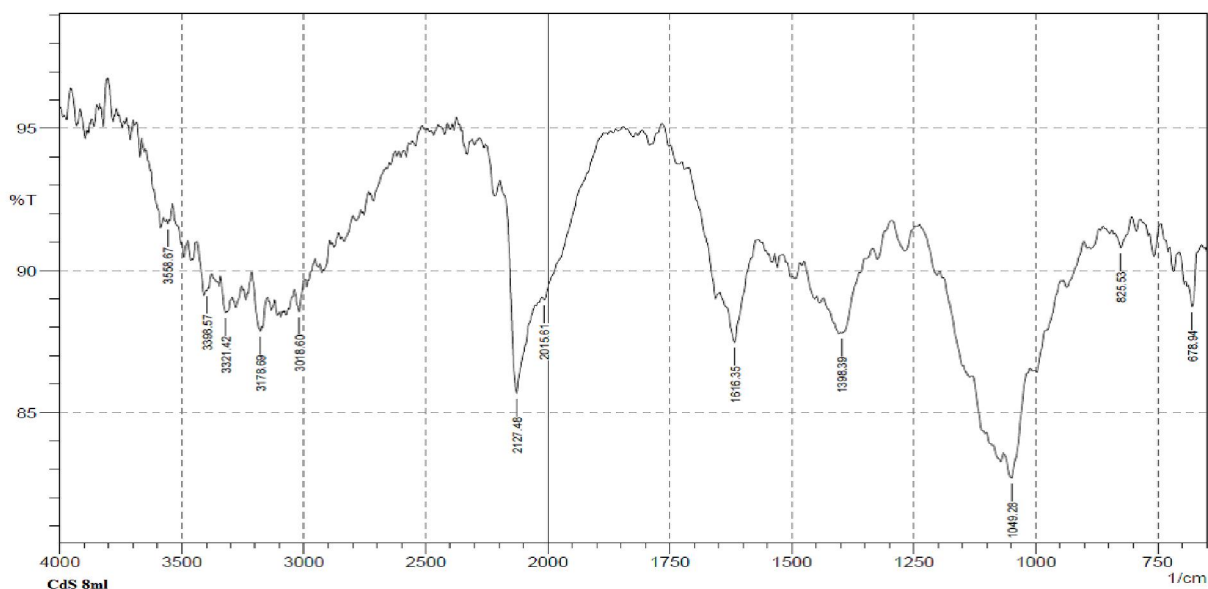


Figure 8 FTIR Pattern of CdS3 Quantum dots

FT-IR spectrum of CdS film is presented in figure 8 the band at 3558.67cm^{-1} is due to O-H stretching vibrations of water molecules. The bending vibrations of C=N appeared at 1616.35cm^{-1} . CdS particles showed two stretching bands of C-O at 1049.28cm^{-1} . At 678.94cm^{-1} and 825.53cm^{-1} , there are medium to strong bands which have been assigned to Cd-S stretching.

3. Conclusion

We prepared Cadmium Sulfide nanoparticles by precipitation method the resulted samples were analyzed by XRD, PL, UV Absorption, and FTIR techniques. The Cadmium sulfide was obtained as uniform, fine and spherical particles.

In, summary CdS Quantum Dots have been successfully studied. The size of CdS nanoparticles is smaller than Bohr radius so that, there is strong quantum confinement. The average crystallite size of the sample was calculated using Scherrer equation. CdS nanoparticles can be prepared using simple precipitation or by sol gel hydrothermal synthesis etc.

The XRD analysis shows that the nanoparticles have the cubic structure and the particle size increase with growth temperature and decrease with concentration of precursor. Texture coefficient represents the preferred orientation. It can be seen that highest texture coefficient in (111) plane, it shows the tendency of (111) orientation.

The absorption of ultra violet or visible radiation results from excitation of bonding electrons as a consequence, the wavelength of absorption peaks can be correlated with the type of bonds in the species hence UV visible absorption spectroscopy is an efficiencies techniques to monitor the optical properties of quantum size particles.

The spectrum exhibits a well-defined absorption peak at 451.84nm for CdS1, 339.79nm for CdS2 and 315.74nm for CdS3; which is considerably blue shifted related to the peak absorption of the bulk cadmium sulfide indicating quantum size effect. The UV absorbance spectral reveal that as the size of the Nanocrystals shrink, the maximum peak shifted to a shorter wavelength leading to corresponding increase in the confinement energies because the valence band is move downward and conduction band is pushed upward thus widening the band gap of the semiconductor Nano crystals. The net effect is that the band gap increases. This results to a blue-shift of the (band-band) excitation energy of the semiconductor. The value of the band gaps of the various synthesized nanoparticles was quite large when compared to typical band gap in bulk CdS. This rapid increase in band gap and shift in the electron transition to higher energies with decreasing dot size is due to enhancement in surface/volume ratio and accompanied increase in oscillation strength of the Nano crystal induced by the quantum size effect (QSE).

Nanoparticle with varying band gaps and diameter emerge in the process. The coloration of the nanoparticle is directly linked to the band gap. The color of the emitted light depends on the size of the quantum dots, the larger the QDT size, the redder the light.

The functional groups present in the synthesized CdS materials are identified by FTIR analysis.

Also study the purity and composition of the materials.

References

1. Q. Wang, G. Xu, G. Han, *J. Solid State Chem.* 178, 2680(2005).
2. A. Morales-Acevedo, *Solar Energy Materials and Solar Cells* 90, 2213(2006).
3. V. Singh, P. Chauhan, (2009) *Chalcogenide Letters* 6, 421. S. Prabakar, N. Suryanarayanan, D. Kathirvel, *Chalcogenide Letters* 6, 577(2009).
4. I.O. Oladeji, L. Chow, J. R. Liu, W. K. Chu, A. N. P. Bustamante, C. Fredricksen, A. F. Schulte, *Thin Solid Films* 359, 154 (2000).
5. M. J. Pawar, S. S. Chaurse, *Chalcogenide Letters* 6, 689(2009).
6. A. Dumbrava, V. Ciupina, G. Prodan, *Proceedings of 4th Aeg. Anal. Chem. Days, Turkey* pp 481 (2004).
7. G. Li, L. Jianga, H. Penga, B. Zhanga, *Mater. Lett.* 62, 1881(2008).
8. X. Liu, *Mat. Chem. Phys.* 91, 212(2005).
9. H. Zhang, D. Yang, X. Ma, Y. Ji, S. Z. Li, D. Que, *Mat. Chem. Phys.* 93, 65(2005).
10. Q. Zhang, F. Huang, Y. Li, *Coll. Surf. A*, 257 – 258, 497(2005).
11. A. Vadivel Murugan, R. S. Sonawane, B. B. Kale, S. K. Apte, A. V. Kulkarni, *Mat. Chem. Phys.* 71, 98, (2001).
12. M. Maleki, Sh. Mirdamadi, R. Ghasemzadeh, M. Sasani Ghamsari, (2008).
13. *Mat. Lett.* 62, (1993).
14. Halperin, W. P., "Quantum size effects in metal particles," *Rev. Mod. Phys.*, Vol. 58, No. 3., pp. 533-607(1986).
15. Lippens, P. E. and Lannoo, M., "Calculation of the band gap for small CdS and ZnS crystallites," *Phys. Rev. B*, Vol. 39, No. 15, pp. 10935- 10942(1989).
16. Chauhan et al., J "Synthesis and characterization of Ni and Cu doped ZnO" *Nanomed Nanotechnol* vol. 8:2(2017).
17. Wang, Y. and Herron, N., "Quantum size effects on the exciton energy of CdS clusters," *Phys. Rev. B*, Vol. 42, No. 11, pp. 7253-7255(1990).
18. Narayanan, S. S. and Pal, S. K., "Aggregated CdS Quantum Dots: Host of Biomolecular Ligands," *J. Phys. Chem. B*, Vol. 110, pp. 24403- 24409(2006).
19. Mthethwa, T., Pullabhotla, V. S. R. R., Mdluli, P. S., Smith, J. W. and Revaprasadu, N., "Synthesis of hexadecylamine capped CdS nanoparticles using heterocyclic cadmium dithiocarbamates as single source precursors," *Polyhedron*, Vol. 28, pp. 2977-2982(2009).
20. Li, C., Liu, Z. and Yang, Y., "The selective synthesis of single-crystalline CdSnanobelts and nanowires by thermal evaporation at lower

- temperature”, *Nanotechnology*, Vol. 17, pp. 1851-1857(2006).
21. Acevedo, A. M., “Can we improve the record efficiency of CdS/CdTe solar cells?,” *Sol. Energy Mater. & Sol. Cells*, Vol. 90, No. 15, pp. 2213-2220(2006).
 22. Lin, C. F., Lianga, E. Z., Shih, S. M. and Si, W. F., “CdS-nanoparticle light-emitting diode on Si,” 119 *Proc. SPIE.*, Vol. 4641, pp. 102-110(2002).
 23. Murai, H., Abe, T., Matsuda, J., Sato, H., Chiba, S. and Kashiwaba, Y., “Improvement in the light emission characteristics of CdS: Cu/CdS diodes,” *Appl. Surf. Sci.*, Vol. 244, pp. 351-354(2005).
 24. Duan, X., Huang, Y., Agarwal, R. and Lieber, C. M., “Single-nanowire electrically driven lasers,” *Nature*, Vol. 421, pp. 241-245(2003).
 25. Zhong, Z., Qian, F., Wang, D. and Lieber, C. M., “Synthesis of p-Type Gallium nitride nanowires for electronic and photonic nanodevices,” *Nano Lett.*, Vol. 3, No. 3, pp. 343-346(2003).
 26. Dai, G., Zou, B. and Wang, Z., “Preparation and periodic emission of superlattice CdS/CdS: SnS₂ Microwires,” *J. Am. Chem. Soc.*, Vol. 132, pp. 12174-12175(2010).
 27. Sejdic, J. T., Peng, H., Cooney, R. P., Bowmaker, G. A., Cannell, M. B. and Soeller, C., “Amplification of a conducting polymer-based DNA sensor signal by CdS nanoparticles,” *Curr. Appl. Phys.*, Vol. 6, pp. 562-566(2006).
 28. Li, X., Jia, Y., Wei, J., Zhu, H., Wang, K., Wu, D. and Cao, A., “solar cells and light sensors based on nanoparticle-grafted carbon nanotube films,” *Acc Nano*, Vol. 4, No. 4, pp. 2142-2148(2010).
 29. Wang, Y., Ramanathan, S., Fan, Q., Yun, F., Morkoe, H. and Bandyopadhyay, S., “Electric field modulation of infrared absorption at room temperature in electrochemically self assembled quantum dots,” *J. Nanosci. Nanotechnol.*, Vol. 6, No. 7, pp. 2077-2080(2006).
 30. Romeoa, N., Bosioa, A., Mazzamutoa, S., Romeob, A. and Vaillant-Rocac, L., “High efficiency cdte/cds thin film solar cells with a novel back-contact,” In *Proceedings of 22nd European Photovoltaic Solar Energy Conference*, Milan, Italy, 3-7 September, pp. 1919-1921(2007).
 31. Zyoud, A. H., Zaatar, N., Saadeddin, I., Ali, C., Park, D., Campet, G. and Hilal, H. S., “CdS sensitized TiO₂ in phenazopyridine photo degradation: Catalyst efficiency, stability and feasibility assessment,” *J. Hazard. Mater.*, Vol. 173, pp. 318-325(2010).
 32. Zhu, H., Jiang, R., Xiao, L., Chang, Y., Guan, Y., Li, X. and Zeng, G., “Photocatalytic decolorization and degradation of Congo Red on innovative crosslinked chitosan/nano-CdS composite catalyst under visible light irradiation,” *J. Hazard. Mater.*, Vol. 169, pp. 933-940(2009).
 33. Acharya, K. P., *Photocurrent Spectroscopy of CdS/plastic, CdS/glass, and ZnTe/GaAs heterostructures formed with pulsed-laser deposition*, Ph.D. Dissertation, Graduate College of Bowling Green State University, (2009).
 34. 26. Yang, Y. J., He, L. Y. and Xiang, H., “Electrochemical synthesis of free-standing CdS nanoparticles in ethylene glycol,” *Russ. J. Electrochem.*, Vol. 42, No. 9, pp. 954-958(2006).
 35. Mathew, X., Sebastian, P. J., Sanchez, A. and Campos, J., “Structural and opto-electronic properties of electrodeposited CdTe on stainless steel foil - photovoltaic energy conversion,” *Sol. Energy Mater. & Sol. Cells*, Vol. 59, No. 16, pp. 99-114(1999).
 36. Barote, M. A., Yadav, A. A., Deshmukh, L. P. and Masumdar, E. U., “Synthesis And Characterization of Chemically Deposited Cd_{1-x}Pb_xS Thin Films,” *J. Non-Oxide Glasses*, Vol. 2, No. 3, pp.151-165(2010).
 37. 29. Martinez-Castanon, G. A., Sanchez-Loredo, M. G., Martinez-Mendoza, J. R. and Ruiz, F., “Synthesis of CdS nanoparticles: a simple methoin aqueous media,” *AZojomo*, Vol. 1, pp.1-7(2005).
 38. Brus, L., “Electronic wave functions in semiconductor clusters: experiment and theory,” *J. Phys. Chem.*, Vol. 90, pp. 2555-2560 (1986).
 39. Brus Equation [Online]. From Wikipedia, the free encyclopedia. <http://en.wikipedia.org/w/index.php?oldid=433920424> (accessed on July 2, 2011).
 40. Baset, S., Akbarib, H., Zeynali, H. and Shafie, M., “Size measurement of metal and semiconductor nanoparticles via UV-Vis absorption spectra,” *Dig. J. Nanomater. Bios.*, Vol. 6, No. 2, pp. 709-716(2011).
 41. A.P. Alivisatos, *Semicond. Clusters Sci.* 271 (5251),933 (1996).
 42. M. A. Hines, and P. Guyot-Sionnest, *J. Phys. Chem.*100 (2), 468 (1996).